

# Newtonian and General Relativistic Models of Spherical Shells - II

D. Vogt\*

P. S. Letelier†

Departamento de Matemática Aplicada-IMECC, Universidade Estadual de Campinas 13083-970 Campinas, São Paulo, Brazil

June 14, 2010

## Abstract

A family of potential-density pairs that represent spherical shells with finite thickness is obtained from the superposition of spheres with finite radii. Other families of shells with infinite thickness with a central hole are obtained by inversion transformations of spheres and of the finite shells. We also present a family of double shells with finite thickness. All potential-density pairs are analytical and can be stated in terms of elementary functions. For the above-mentioned structures, we study the circular orbits of test particles and their stability with respect to radial perturbations. All examples presented are found to be stable. A particular isotropic form of a metric in spherical coordinates is used to construct a General Relativistic version of the Newtonian families of spheres and shells. The matter of these structures is anisotropic, and the degree of anisotropy is a function of the radius.

**Key words:** gravitation – galaxies: kinematics and dynamics.

## 1 Introduction

Analytical potential-density pairs with spherical symmetry have played an important role in galactic dynamics. Simplified models may be used not only to test and to perform sophisticated numerical simulations, but also to help us gain insight into more complicated phenomena. Several spherical analytical potential-density pairs have been proposed as models for elliptical galaxies and bulges of disc galaxies [1, 2, 3], for dark matter haloes [4], as well as generalizations of these models [5, 6, 7]. Shells constitute another spherical self-gravitating system that is important in issues like cosmology, gravitational collapse and supernovae (see, for instance, [8] and references therein). A common simplification

---

\*e-mail: dvogt@ime.unicamp.br

†e-mail: letelier@ime.unicamp.br

is to consider shells with infinitesimal thickness. Rein [9] constructed analytic solutions of the Vlasov-Poisson and Vlasov-Einstein systems representing, respectively, Newtonian and General Relativistic shells with finite thickness and a vacuum at the centre. A more detailed analysis of relativistic shells was done by [10]. Solutions for relativistic double and also multishells were found by [11] using numerical methods. Other numerical solutions of finite Vlasov-Einstein shells were obtained by [12]. Recently, [13] proposed a simple Newtonian family of potential-density pairs of spherical shells with varying thicknesses and also a General Relativistic version of these models.

In this work, we obtain families of potential-density pairs that represent spherical shells with finite thickness and shells with infinite thickness that have a central hole. We also build a family of double shells with finite thickness. For these structures, we study the rotation curves (circular orbits) of test particles and make a first stability analysis by considering the stability of circular orbits under small radial perturbations. We also consider a General Relativistic version of some of these Newtonian potential-density pairs in the same manner as in our previous work [13]. The paper is divided as follows. In Section 2, we present a family of spheres with finite radii that will be used as a basis for the construction of the spherical shells. In Section 3, the inversion theorem is applied on the spheres to obtain a first family of infinite shells. Then, in Section 4, shells with finite thickness are constructed by superposing different members of the family of spheres. The inversion theorem is also used on these shells to obtain another family of infinite shells with a central hole. In Section 5, we show how to construct a family of double shells with finite thickness by superposing different members of finite shells, and we discuss a particular example. In Section 6, we use a particular isotropic form of a metric in spherical coordinates to construct a simple General Relativistic version of the Newtonian spheres and shells. We study in some detail two examples of spherical structures. Finally, in Section 7 we summarize our results.

## 2 A family of finite spheres

We begin by considering a family of spheres with finite radius and following mass-density distribution,

$$\rho_m = \begin{cases} \rho_c \left(1 - \frac{r^2}{a^2}\right)^{m-1/2}, & 0 \leq r \leq a, \\ 0, & r > a, \end{cases} \quad (1)$$

where  $m = 1, 2, \dots$ . This form of mass distribution has been chosen because it is a monotonically decreasing function of the radius and the corresponding potential can be expressed in terms of elementary functions, as will be seen below. Furthermore, models of thin finite discs with surface densities in the form of (1), where  $r$  now represents the cylindrical radius, are well known. The disc member with  $m = 1$  is the uniformly rotating disc of Kalnajs [14]. González & Reina [15] constructed a family of generalized Kalnajs discs with

surface density similar to (1); however, it is interesting to note that a family of discs with a similar density distribution has been used much earlier by Morgan & Morgan [16] in their study of General Relativistic static thin discs.

The total mass  $M_m$  of the sphere is

$$M_m = 4\pi \int_0^a r^2 \rho_m dr = \frac{\rho_c \pi^2 a^3 (2m-1)!!}{2^m (m+1)!}. \quad (2)$$

For convenience, we consider spheres with the same mass  $M = M_m$ . Then, equation (1) can be rewritten as

$$\rho_m = \frac{M 2^m (m+1)!}{\pi^2 a^3 (2m-1)!!} \left(1 - \frac{r^2}{a^2}\right)^{m-1/2}. \quad (3)$$

The potential of the sphere with  $m = 1$  follows from direct integration of the Poisson equation in spherical coordinates:

$$\frac{1}{r^2} \frac{d}{dr} \left( r^2 \frac{d\Phi}{dr} \right) = 4\pi G \rho, \quad (4)$$

and is given by

$$\Phi_1 = \begin{cases} -\frac{2GM}{3\pi a^4} \left[ \frac{3a^4}{r} \arcsin\left(\frac{r}{a}\right) - \sqrt{a^2 - r^2} (2r^2 - 5a^2) \right], & 0 \leq r \leq a, \\ -\frac{GM}{r}, & r > a. \end{cases} \quad (5)$$

The potentials of the spheres with  $m > 1$  can be found by using the recurrence relation

$$\Phi_{m+1} = \frac{2m+4}{a^{2m+4}} \int a^{2m+3} \Phi_m da. \quad (6)$$

For reference, the potentials of the members with  $m = 2, 3, 4$  read as

$$\Phi_2 = -\frac{2GM}{15\pi a^6} \left[ \frac{15a^6}{r} \arcsin\left(\frac{r}{a}\right) + \sqrt{a^2 - r^2} (8r^4 - 26a^2 r^2 + 33a^4) \right], \quad (7)$$

$$\Phi_3 = -\frac{2GM}{105\pi a^8} \left[ \frac{105a^8}{r} \arcsin\left(\frac{r}{a}\right) - \sqrt{a^2 - r^2} (48r^6 - 200r^4 a^2 + 326r^2 a^4 - 279a^6) \right], \quad (8)$$

$$\Phi_4 = -\frac{2GM}{315\pi a^{10}} \left[ \frac{315a^{10}}{r} \arcsin\left(\frac{r}{a}\right) + \sqrt{a^2 - r^2} (128r^8 - 656r^6 a^2 + 1368r^4 a^4 - 1490r^2 a^6 + 965a^8) \right]. \quad (9)$$

A common dynamical quantity used to characterize spherical distributions of matter is the circular velocity  $v_c$  (or the rotation curve) of test particles. We will mostly be interested in the circular orbits of particles inside the matter distributions. We also investigate the stability of these orbits under small radial perturbations. This is characterized by the epicyclic frequency  $\kappa$ , where stable

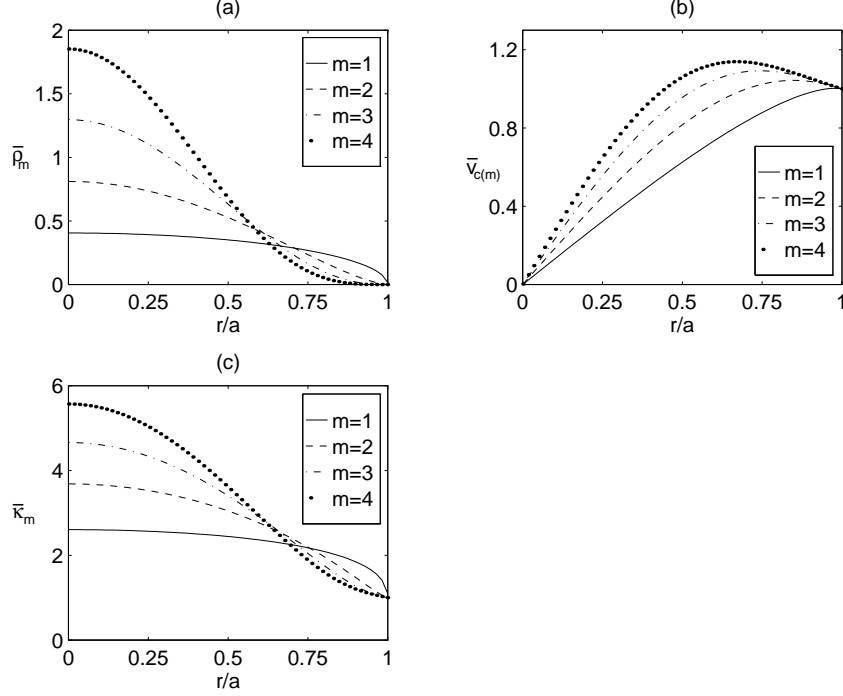


Figure 1: (a) The mass density  $\bar{\rho}_m = \rho_m/(M/a^3)$ , equation (3), as function of  $r/a$ , for four members of spheres. (b) The circular velocity  $\bar{v}_{c(m)} = v_{c(m)}/(GM/a)^{1/2}$ , equations (46)–(49), and (c) the epicyclic frequency  $\bar{\kappa}_m = \kappa_m/(GM/a^3)^{1/2}$ , equations (50)–(53), as functions of  $r/a$ , for the same members of spheres.

circular orbits correspond to  $\kappa^2 > 0$ . For spherical potentials, the circular velocity and epicyclic frequency are calculated through the relations [17]

$$v_c = \sqrt{r\Phi_{,r}}, \quad \text{and} \quad \kappa^2 = \Phi_{,rr} + \frac{3\Phi_{,r}}{r}. \quad (10)$$

Expressions for the circular velocity  $v_{c(m)}$  and epicyclic frequency  $\kappa_m$  for the spheres with  $m = 1, 2, 3, 4$  are listed in Appendix A. Outside the spheres ( $r > a$ ), we have  $v_c = (GM/r)^{1/2}$  and  $\kappa = (GM/r^3)^{1/2}$ .

In Fig. 1(a), we plot some curves of the dimensionless mass density  $\bar{\rho}_m = \rho_m/(M/a^3)$ , equation (3), as function of  $r/a$ , for four members of the family of spheres. In Figs 1(b) and (c) we show, respectively, some curves of the dimensionless circular velocity  $\bar{v}_{c(m)} = v_{c(m)}/(GM/a)^{1/2}$ , equations (46)–(49), and curves of the dimensionless epicyclic frequency  $\bar{\kappa}_m = \kappa_m/(GM/a^3)^{1/2}$ , equations (50)–(53), as functions of  $r/a$ , for four members of the family of spheres. Unlike the disc case, we do not have a linear rotation profile for the sphere with  $m = 1$ . We also note that the circular orbits for the four first members are

stable.

### 3 Inverted spheres

A new family of spherical potential density-pairs can be obtained by making an inversion (or a Kelvin transformation) [18, 19] on the spheres with density (3). In spherical coordinates, the inversion theorem states that if a potential-density pair  $\rho(r)$ ,  $\Phi(r)$  is a solution to the Poisson equation, then the pair

$$\rho_{(inv.)} = \left(\frac{a}{r}\right)^5 \rho\left(\frac{a^2}{r}\right), \quad (11)$$

$$\Phi_{(inv.)} = \frac{a}{r} \Phi\left(\frac{a^2}{r}\right), \quad (12)$$

is also a solution to the Poisson equation. The inversion theorem applied to the density (3) results in

$$\rho_{m(inv.)} = \frac{M2^m a^2 (m+1)!}{\pi^2 r^5 (2m-1)!!} \left(1 - \frac{a^2}{r^2}\right)^{m-1/2}, \quad r \geq a. \quad (13)$$

This mass distribution can be interpreted as a family of spherical shells with a central hole of radius  $a$ . The shells extend to infinity, although the density decays quite fast,  $\rho_{m(inv.)} \propto 1/r^5$ . The maximum of density occurs at  $r/a = \sqrt{(2m+4)/5}$ . The mass  $\mathcal{M}_m$  of each shell is

$$\mathcal{M}_m = 4\pi \int_a^\infty r^2 \rho_{m(inv.)} dr = \frac{M2^{m+2}(m+1)!}{\pi(2m+1)(2m-1)!!}. \quad (14)$$

For convenience, we consider shells with the same mass  $\mathcal{M} = \mathcal{M}_m$  and rewrite (13) as

$$\rho_{m(inv.)} = \frac{(2m+1)\mathcal{M}a^2}{4\pi r^5} \left(1 - \frac{a^2}{r^2}\right)^{m-1/2}, \quad r \geq a. \quad (15)$$

The expressions for the potentials of the shells with  $m = 1, 2, 3, 4$  are given in Appendix B. From them result simple equations for the rotation curves

$v_{c(m)(inv.)}$  and epicyclic frequencies  $\kappa_{m(inv.)}$ , namely

$$v_{c(1)(inv.)} = \sqrt{\frac{GM}{r}} \left(1 - \frac{a^2}{r^2}\right)^{3/4}, \quad v_{c(2)(inv.)} = \sqrt{\frac{GM}{r}} \left(1 - \frac{a^2}{r^2}\right)^{5/4}, \quad (16)$$

$$v_{c(3)(inv.)} = \sqrt{\frac{GM}{r}} \left(1 - \frac{a^2}{r^2}\right)^{7/4}, \quad v_{c(4)(inv.)} = \sqrt{\frac{GM}{r}} \left(1 - \frac{a^2}{r^2}\right)^{9/4}, \quad (17)$$

$$\kappa_{1(inv.)} = \sqrt{\frac{GM(r^2 + 2a^2)}{r^5}} \left(1 - \frac{a^2}{r^2}\right)^{1/4}, \quad (18)$$

$$\kappa_{2(inv.)} = \sqrt{\frac{GM(r^2 + 4a^2)}{r^5}} \left(1 - \frac{a^2}{r^2}\right)^{3/4}, \quad (19)$$

$$\kappa_{3(inv.)} = \sqrt{\frac{GM(r^2 + 6a^2)}{r^5}} \left(1 - \frac{a^2}{r^2}\right)^{5/4}, \quad (20)$$

$$\kappa_{4(inv.)} = \sqrt{\frac{GM(r^2 + 8a^2)}{r^5}} \left(1 - \frac{a^2}{r^2}\right)^{7/4}, \quad (21)$$

which suggest the general relations

$$v_{c(m)(inv.)} = \sqrt{\frac{GM}{r}} \left(1 - \frac{a^2}{r^2}\right)^{(2m+1)/4}, \quad (22)$$

$$\kappa_{m(inv.)} = \sqrt{\frac{GM(r^2 + 2ma^2)}{r^5}} \left(1 - \frac{a^2}{r^2}\right)^{(2m-1)/4}. \quad (23)$$

Some curves of the dimensionless mass density  $\bar{\rho}_{m(inv.)} = \rho_{m(inv.)}/(\mathcal{M}/a^3)$ , equation (15), as function of  $r/a$ , are shown in Fig. 2(a). The shell with  $m = 1$  exhibits a quite sharp density profile. In Figs 2(b) and (c), we plot, respectively, curves of the dimensionless circular velocity  $\bar{v}_{c(m)(inv.)} = v_{c(m)(inv.)}/(GM/a)^{1/2}$ , equations (16) and (17), and the dimensionless epicyclic frequency  $\bar{\kappa}_{m(inv.)} = \kappa_{m(inv.)}/(GM/a^3)^{1/2}$ , equations (18)–(21), as functions of  $r/a$ . The four members of the shells shown are stable with respect to radial perturbations of circular orbits. From (23), we see that all members are stable. According to Newton's shell theorem, the potential inside the hole ( $0 \leq r \leq a$ ) is constant and thus the circular velocity must be zero.

## 4 Families of spherical shells

Now we use the spheres discussed in Section 2 to construct potential-density pairs that represent shells of matter with finite thickness. The method is similar to the used by [20] to obtain rings by superposing the Morgan & Morgan discs

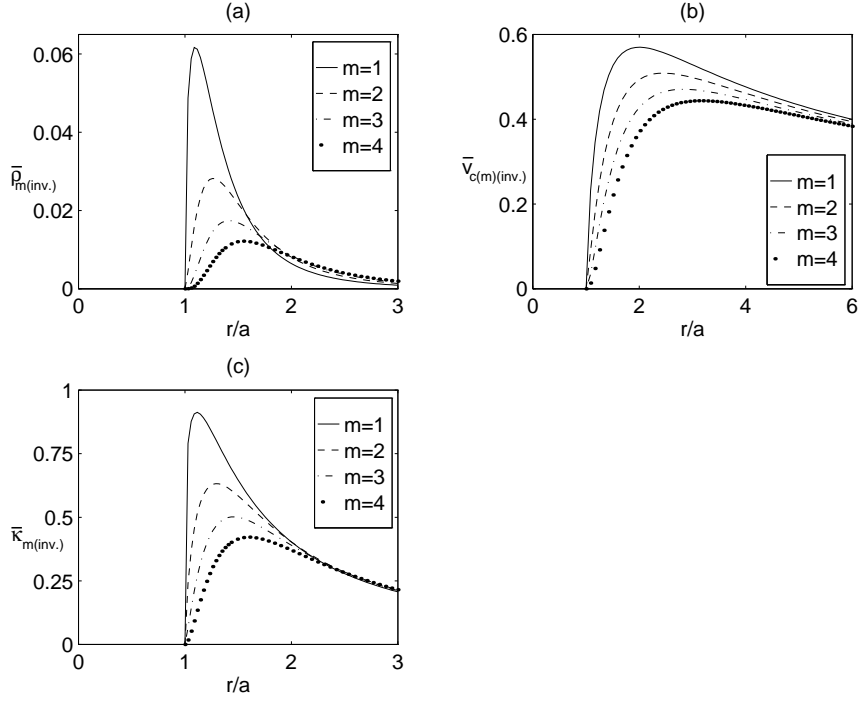


Figure 2: (a) The mass density  $\bar{\rho}_{m(inv.)} = \rho_{m(inv.)}/(\mathcal{M}/a^3)$ , equation (15), as function of  $r/a$ , for four members of inverted spheres. (b) The circular velocity  $\bar{v}_{c(m)(inv.)} = v_{c(m)(inv.)}/(G\mathcal{M}/a)^{1/2}$ , equations (16) and (17), and (c) the epicyclic frequency  $\bar{\kappa}_{m(inv.)} = \kappa_{m(inv.)}/(G\mathcal{M}/a^3)^{1/2}$ , equations (18)–(21), as functions of  $r/a$ , for the same members of inverted spheres.

[16]. We take the density distribution (1) and make the following sum:

$$\begin{aligned}\rho^{(m,n)} &= \sum_{k=0}^n C_k^m (-1)^{n-k} \rho_{m+n+1-k} \\ &= \rho_c \left(1 - \frac{r^2}{a^2}\right)^{m+1/2} \sum_{k=0}^n C_k^m (-1)^{n-k} \left(1 - \frac{r^2}{a^2}\right)^{n-k} = \rho_c \left(1 - \frac{r^2}{a^2}\right)^{m+1/2} \left(\frac{r}{a}\right)^{2n},\end{aligned}\quad (24)$$

where  $C_k^m = n!/[k!(n-k)!]$ ,  $m = 0, 1, \dots$  and  $n = 1, 2, \dots$ . This new density distribution vanishes on  $r = 0$  and  $r = a$ , so it represents a spherical shell with thickness  $a$ . Its mass density has a maximum value at  $r/a = \sqrt{(2n)/(2m+2n+1)}$ . The total mass  $M^{(m,n)}$  of each shell is

$$M^{(m,n)} = 4\pi \int_0^a r^2 \rho^{(m,n)} dr = \frac{\rho_c \pi^2 a^3 (2m+1)!! (2n+1)!!}{2^{m+n+1} (m+n+2)!}. \quad (25)$$

The potentials associated with the mass density (24) are found by a similar sum, i.e. the potential of the shell with  $m = 0, n = 1$  is  $\Phi^{(0,1)} = \Phi_1 - \Phi_2$ . The explicit expressions for the potentials of the shells with  $m = 0, 1$  and  $n = 1, 2$  are given in Appendix C.

In Fig. 3(a), we display curves of the dimensionless mass density  $\bar{\rho}^{(m,n)} = \rho^{(m,n)}/\rho_c$ , equation (24), as function of  $r/a$ , for four members of spherical shells. For small values of  $r/a$ , the density of the shell grows as  $(r/a)^{2(n+1)}$ ; therefore, shells with larger values of  $n$  also have larger holes. Curves of the dimensionless circular velocity  $\bar{v}_c^{(m,n)} = v_c^{(m,n)}/(G\rho_c a^2)^{1/2}$ , equations (62)–(65), and of the dimensionless epicyclic frequency  $\bar{\kappa}^{(m,n)} = \kappa^{(m,n)}/(G\rho_c)^{1/2}$ , equations (66)–(69), are displayed in Figs 3(b) and (c), respectively. For small values of  $r/a$ , the rotation curves are proportional to  $(r/a)^{n+2}$  and thus also grow more slowly as  $n$  increases. We also see that the members of shells shown in the figure are stable.

It is also possible to invert the shells. A Kelvin transformation applied to the density (24) results in

$$\rho_{(inv.)}^{(m,n)} = \rho_c \left(1 - \frac{a^2}{r^2}\right)^{m+1/2} \left(\frac{a}{r}\right)^{2n+5}; \quad r \geq a, \quad (26)$$

which represents a shell with a central hole of radius  $a$ . If  $n = 0$  and  $m \rightarrow m-1$  we recover the family of inverted shells discussed in Section 3. They also extend to infinity with an even larger decay of density,  $\rho_{(inv.)}^{(m,n)} \propto 1/r^{2n+5}$ . The maximum of density occurs at  $r/a = \sqrt{(2m+2n+6)/(2n+5)}$ . The total mass of each shell is

$$4\pi \int_a^\infty r^2 \rho_{(inv.)}^{(m,n)} dr = \frac{\rho_c \pi a^3 2^{n+2} n! (2m+1)!!}{(2m+2n+3)!}. \quad (27)$$

Curves of the dimensionless mass density  $\bar{\rho}_{(inv.)}^{(m,n)}$ , equation (26), as function of  $r/a$ , are displayed in Fig. 4(a) for four members of inverted shells. Figs



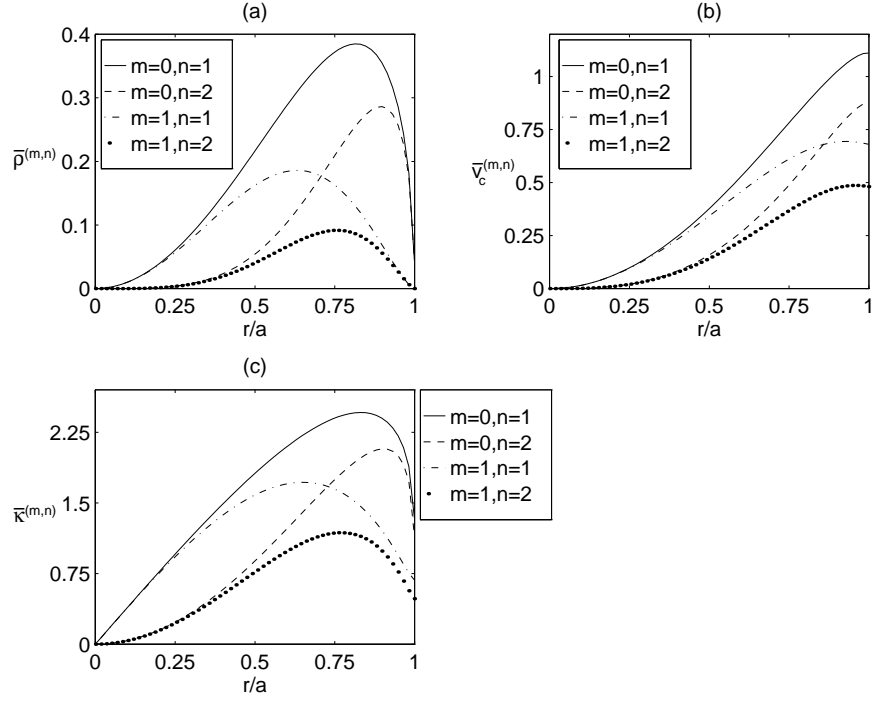


Figure 3: (a) The mass density  $\bar{\rho}^{(m,n)} = \rho^{(m,n)}/\rho_c$ , equation (24), as function of  $r/a$ , for four members of spherical shells. (b) The circular velocity  $\bar{v}_c^{(m,n)} = v_c^{(m,n)}/(G\rho_c a^2)^{1/2}$ , equations (62)–(65), and (c) the epicyclic frequency  $\bar{\kappa}^{(m,n)} = \kappa^{(m,n)}/(G\rho_c)^{1/2}$ , equations (66)–(69), as functions of  $r/a$ , for the same members of spherical shells.

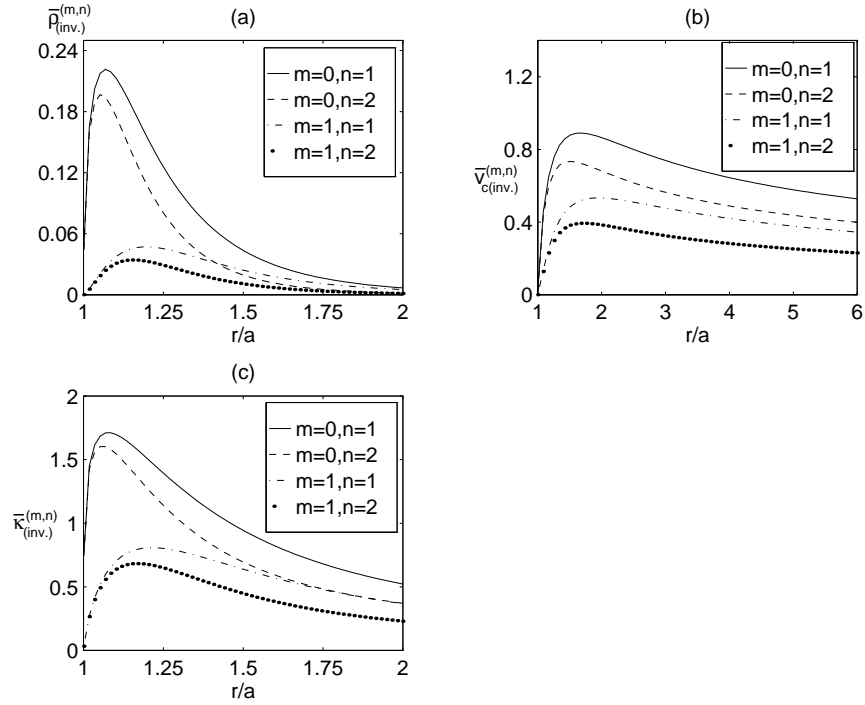


Figure 4: (a) The mass density  $\bar{\rho}_{(inv.)}^{(m,n)} = \rho_{(inv.)}^{(m,n)}/\rho_c$ , equation (26), as function of  $r/a$ , for four members of inverted shells. (b) The circular velocity  $\bar{v}_{c(inv.)}^{(m,n)} = v_{c(inv.)}^{(m,n)}/(G\rho_c a^2)^{1/2}$ , equations (74)–(77), and (c) the epicyclic frequency  $\bar{\kappa}_{(inv.)}^{(m,n)} = \kappa_{(inv.)}^{(m,n)}/(G\rho_c)^{1/2}$ , equations (78)–(81), as functions of  $r/a$ , for the same members of inverted shells.

4(b) and (c) show, respectively, curves of the dimensionless circular velocity  $\bar{v}_{c(inv.)}^{(m,n)}$ , equations (74)–(77), and of the dimensionless epicyclic frequency  $\bar{\kappa}_{(inv.)}^{(m,n)}$ , equations (78)–(81), for the same members of inverted shells. Once again, these members are stable with respect to radial perturbations of circular orbits.

## 5 A family of double shells

The members of the family of shells discussed in Section 4 may be combined to generate double shells with finite thickness. To achieve this, we superpose members of (24) in the following way:

$$\rho_{(2)}^{(m,n)} = \rho^{(m,n)} - 2b^2 \rho^{(m,n+1)} + b^4 \rho^{(m,n+2)} = \rho_c \left(1 - \frac{r^2}{a^2}\right)^{m+1/2} \left(\frac{r}{a}\right)^{2n} \left(1 - \frac{b^2 r^2}{a^2}\right)^2, \quad (28)$$

where  $b > 1$ . This density distribution may be interpreted as two concentric spherical shells with a gap located at  $r/a = 1/b$ . We take as an example the member with  $m = 0, n = 1$ . The potential as well as the expressions of the rotation curve and epicyclic frequency for this example are given in Appendix E.

Fig. 5(a) shows curves of the dimensionless mass density  $\bar{\rho}_{(2)}^{(0,1)} = \rho_{(2)}^{(0,1)} / \rho_c$ , equation (28), as function of  $r/a$  for some values of  $b$ . Curves of the circular velocity  $\bar{v}_{c(2)}^{(0,1)} = v_{c(2)}^{(0,1)} / (G\rho_c a^2)^{1/2}$ , equation (83), and of the epicyclic frequency  $\bar{\kappa}_{(2)}^{(m,n)} = \kappa_{(2)}^{(m,n)} / (G\rho_c)^{1/2}$ , equation (84), are plotted in Figs 5(b) and (c), respectively. Unlike the structures discussed so far, the rotation curves for this example of double shell show a point of minimum. They also show no sign of instability.

## 6 General Relativistic Spheres and Shells

Now we consider an extension to General Relativity of the Newtonian spherical potential-density pairs discussed so far. We choose a particular metric in an isotropic form in spherical coordinates  $(t, r, \theta, \varphi)$ , which was also used in a recent work on another relativistic model of shells [13],

$$ds^2 = \left(\frac{1-f}{1+f}\right)^2 c^2 dt^2 - (1+f)^4 (dr^2 + r^2 d\theta^2 + r^2 \sin^2 \theta d\varphi^2), \quad (29)$$

where  $f = f(r)$ . The Schwarzschild solution is given by metric (29) if  $f = GM/(2c^2 r)$ , and the relation between the function  $f(r)$  and the Newtonian potential  $\Phi(r)$  is

$$f = -\frac{\Phi}{2c^2}. \quad (30)$$

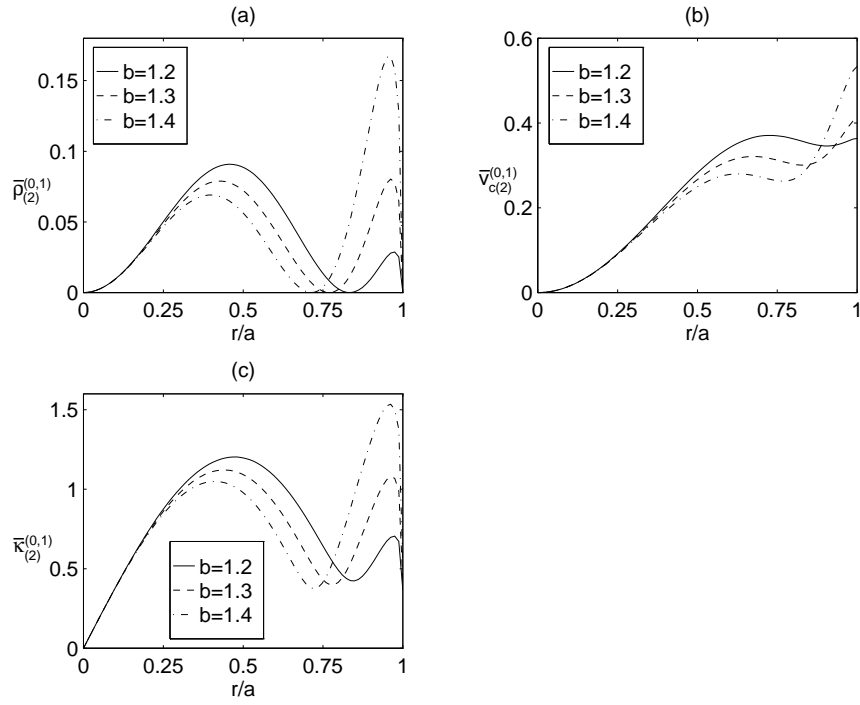


Figure 5: (a) The mass density  $\bar{\rho}_{(2)}^{(0,1)} = \rho_{(2)}^{(0,1)} / \rho_c$ , equation (28), as function of  $r/a$ , for a double shell. (b) The circular velocity  $\bar{v}_{c(2)}^{(0,1)} = v_{c(2)}^{(0,1)} / (G\rho_c a^2)^{1/2}$ , equation (83), and (c) the epicyclic frequency  $\bar{\kappa}_{(2)}^{(m,n)} = \kappa_{(2)}^{(m,n)} / (G\rho_c)^{1/2}$ , equation (84), as functions of  $r/a$ , for the same double shell.

By using the Einstein equations, we find the following expressions for the non-zero components of the energy-momentum tensor  $T_{\mu\nu}$  [13]

$$T_t^t = -\frac{c^4}{2\pi G(1+f)^5} \frac{1}{r^2} \frac{d}{dr} \left( r^2 \frac{df}{dr} \right), \quad (31)$$

$$T_r^r = \frac{c^4}{2\pi G(1+f)^5(1-f)} \frac{df}{dr} \left( \frac{f}{r} + \frac{df}{dr} \right), \quad (32)$$

$$T_\theta^\theta = T_\varphi^\varphi = \frac{c^4}{4\pi G(1+f)^5(1-f)} \left[ f \frac{d^2 f}{dr^2} + \frac{f}{r} \frac{df}{dr} - \left( \frac{df}{dr} \right)^2 \right]. \quad (33)$$

The energy density reads as  $\epsilon = T_t^t/c^2$  and the pressures or tensions along a direction  $k$  are given by  $P_k = -T_k^k$ . The ‘effective Newtonian density’  $\rho_N = \epsilon + P_r/c^2 + P_\theta/c^2 + P_\varphi/c^2$  can be cast as

$$\rho_N = -\frac{c^2}{2\pi G(1+f)^5(1-f)} \frac{1}{r^2} \frac{d}{dr} \left( r^2 \frac{df}{dr} \right). \quad (34)$$

We will study in some detail two simple examples of General Relativistic spherical structures with finite extent: the sphere with potential (5) and the shell with potential (58). Using equations (5) and (30)–(34), we find the following expressions for the components of the energy-momentum tensor of the sphere,

$$\tilde{\epsilon}_1 = \frac{4}{\pi^2 \tilde{a}^3 (1+f_1)^5} \sqrt{1 - \frac{\tilde{r}^2}{\tilde{a}^2}}, \quad (35)$$

$$\tilde{\rho}_{N1} = \frac{4}{\pi^2 \tilde{a}^3 (1+f_1)^5 (1-f_1)} \sqrt{1 - \frac{\tilde{r}^2}{\tilde{a}^2}}, \quad (36)$$

$$\begin{aligned} \tilde{P}_{r1} = & \frac{8}{3\pi^3 \tilde{a}^4 \tilde{r}^2 (1+f_1)^5 (1-f_1)} \left( 1 - \frac{\tilde{r}^2}{\tilde{a}^2} \right)^{3/2} \left[ \frac{\tilde{a}^3}{\tilde{r}} \arcsin \left( \frac{\tilde{r}}{\tilde{a}} \right) \right. \\ & \left. + (2\tilde{r}^2 - \tilde{a}^2) \sqrt{1 - \frac{\tilde{r}^2}{\tilde{a}^2}} \right], \end{aligned} \quad (37)$$

$$\begin{aligned} \tilde{P}_{\theta 1} = \tilde{P}_{\varphi 1} = & \frac{4}{3\pi^3 \tilde{a}^4 \tilde{r}^2 (1+f_1)^5 (1-f_1)} \sqrt{1 - \frac{\tilde{r}^2}{\tilde{a}^2}} \left[ \frac{\tilde{a}}{\tilde{r}} (4\tilde{r}^2 - \tilde{a}^2) \arcsin \left( \frac{\tilde{r}}{\tilde{a}} \right) \right. \\ & \left. + (2\tilde{r}^2 + \tilde{a}^2) \sqrt{1 - \frac{\tilde{r}^2}{\tilde{a}^2}} \right], \end{aligned} \quad (38)$$

with

$$f_1 = \frac{2}{3\pi \tilde{a}^4} \left[ \frac{3\tilde{a}^4}{\tilde{r}} \arcsin \left( \frac{\tilde{r}}{\tilde{a}} \right) - \sqrt{\tilde{a}^2 - \tilde{r}^2} (2\tilde{r}^2 - 5\tilde{a}^2) \right], \quad (39)$$

and the dimensionless variables and parameters are  $\tilde{r} = r/r_s$ ,  $\tilde{a} = a/r_s$ ,  $\tilde{\epsilon}_1 = \epsilon_1/(M/r_s^3)$ ,  $\tilde{\rho}_{N1} = \rho_{N1}/(M/r_s^3)$ ,  $\tilde{P}_{k1} = P_{k1}/(Mc^2/r_s^3)$  and  $r_s = GM/(2c^2)$ .

In order to represent physically meaningful matter distributions, the components of the energy-momentum tensor should satisfy the energy conditions.

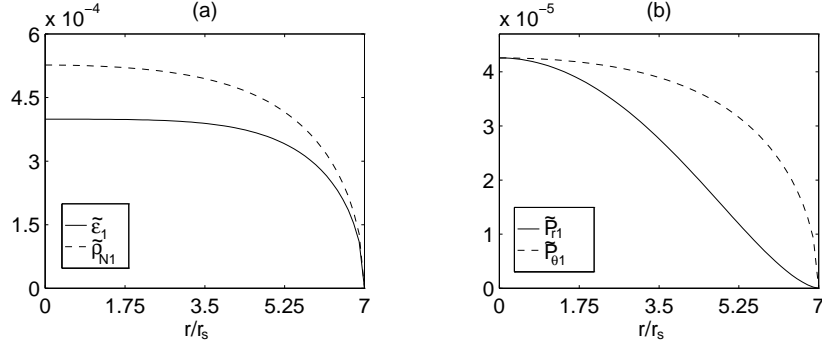


Figure 6: (a) The energy density  $\tilde{\epsilon}_1 = \epsilon_1/(M/r_s^3)$  (solid curve), equation (35), and the effective Newtonian density  $\tilde{\rho}_{N1} = \rho_{N1}/(M/r_s^3)$  (dashed curve), equation (36), for the sphere with radius  $\tilde{a} = 7$ . (b) The radial pressure  $\tilde{P}_{r1} = P_{r1}/(Mc^2/r_s^3)$  (solid curve), equation (37), and the azimuthal/polar pressure  $\tilde{P}_{\theta1} = P_{\theta1}/(Mc^2/r_s^3)$  (dashed curve), equation (38), for the sphere with radius  $\tilde{a} = 7$ .

The strong energy condition states that  $\rho_N \geq 0$ , whereas the weak energy condition imposes the condition  $\epsilon \geq 0$ . The dominant energy condition requires  $|P_k/\epsilon| \leq c^2$ . Equations (35) and (36) show that the strong and weak energy conditions are satisfied if  $\tilde{a} \geq 16/(3\pi) \approx 1.70$ . In Fig. 6(a), we plot the curves of the energy density  $\tilde{\epsilon}_1$  (solid curve) and the effective Newtonian density  $\tilde{\rho}_{N1}$  (dashed curve), as functions of  $\tilde{r} = r/r_s$ , for the sphere with radius  $\tilde{a} = 7$ , and in Fig. 6(b), we display the radial pressure  $\tilde{P}_{r1}$  (solid curve) and the azimuthal/polar pressure  $\tilde{P}_{\theta1}$ , as functions of  $\tilde{r} = r/r_s$ , for the same sphere. Unfortunately, we found that the energy density is not always a monotone decreasing function of the radius. This happens if  $\tilde{a} \lesssim 6.8$ . For  $\tilde{a} \gtrsim 6.8$ , the dominant energy condition is also satisfied. The radial and azimuthal pressures also decrease monotonically and both vanish on the sphere's surface. In this example, we have an anisotropic sphere with larger azimuthal/polar than radial pressures.

In the case of the shell with potential (58), we obtain the following expres-

sions for the components of the energy-momentum tensor:

$$\hat{\epsilon}^{(0,1)} = \frac{1}{[1 + f^{(0,1)}]^5} \left( \frac{\hat{r}}{\hat{a}} \right)^2 \sqrt{1 - \frac{\hat{r}^2}{\hat{a}^2}}, \quad (40)$$

$$\hat{\rho}_N^{(0,1)} = \frac{1}{[1 + f^{(0,1)}]^5 [1 - f^{(0,1)}]} \left( \frac{\hat{r}}{\hat{a}} \right)^2 \sqrt{1 - \frac{\hat{r}^2}{\hat{a}^2}}, \quad (41)$$

$$\begin{aligned} \hat{P}_r^{(0,1)} = & \frac{\pi (3\hat{r}^2 + 2\hat{a}^2)}{360\hat{a}^2\hat{r}^2 [1 + f^{(0,1)}]^5 [1 - f^{(0,1)}]} \left( 1 - \frac{\hat{r}^2}{\hat{a}^2} \right)^{3/2} \left[ \frac{3\hat{a}^5}{\hat{r}} \arcsin \left( \frac{\hat{r}}{\hat{a}} \right) \right. \\ & \left. + (2\hat{r}^2 + \hat{a}^2) (4\hat{r}^2 - 3\hat{a}^2) \sqrt{1 - \frac{\hat{r}^2}{\hat{a}^2}} \right], \end{aligned} \quad (42)$$

$$\begin{aligned} \hat{P}_\theta^{(0,1)} = \hat{P}_\varphi^{(0,1)} = & \frac{\pi}{720\hat{a}^2\hat{r}^2 [1 + f^{(0,1)}]^5 [1 - f^{(0,1)}]} \sqrt{1 - \frac{\hat{r}^2}{\hat{a}^2}} \\ \times & \left[ \frac{3\hat{a}^3}{\hat{r}} (18\hat{r}^4 - \hat{r}^2\hat{a}^2 - 2\hat{a}^4) \arcsin \left( \frac{\hat{r}}{\hat{a}} \right) + (4\hat{r}^6 + 28\hat{r}^4\hat{a}^2 + 7\hat{r}^2\hat{a}^4 + 6\hat{a}^6) \sqrt{1 - \frac{\hat{r}^2}{\hat{a}^2}} \right], \end{aligned} \quad (43)$$

with

$$f^{(0,1)} = \frac{1}{120\hat{a}^3} \left[ \frac{15\hat{a}^6}{\hat{r}} \arcsin \left( \frac{\hat{r}}{\hat{a}} \right) - \sqrt{\hat{a}^2 - \hat{r}^2} (8\hat{r}^4 - 6\hat{a}^2\hat{r}^2 - 17\hat{a}^4) \right], \quad (44)$$

and the dimensionless variables and parameters are now  $\hat{r} = r/r_c$ ,  $\hat{a} = a/r_c$ ,  $\hat{\epsilon}^{(0,1)} = \epsilon^{(0,1)}/\rho_c$ ,  $\hat{\rho}_N^{(0,1)} = \rho_N^{(0,1)}/\rho_c$ ,  $\hat{P}_k^{(0,1)} = P_k^{(0,1)}/(\rho_c c^2)$  and  $r_c = c/\sqrt{G\rho_c}$ .

From equations (40) and (41), we have that the strong and weak energy conditions are satisfied when  $\hat{a} \leq \sqrt{15}/2 \approx 1.94$ . The dominant energy condition holds if

$$\hat{a} \leq \frac{5\sqrt{6\pi + 15}}{2(2\pi + 5)} \approx 1.29. \quad (45)$$

Fig. 7(a) shows curves of the energy density  $\hat{\epsilon}^{(0,1)}$  (solid curve) and the effective Newtonian density  $\hat{\rho}_N^{(0,1)}$  (dashed curve), as functions of  $r/r_c$ , for the shell with parameter  $\hat{a} = 1.2$ . In Fig. 7(b), we show curves of the radial pressure  $\hat{P}_r^{(0,1)}$  (solid curve) and the azimuthal/polar pressure  $\hat{P}_\theta^{(0,1)}$  (dashed curve), as functions of  $r/r_c$ , for the same shell. The pressures, as well as the densities, vanish at the centre and at the outer surface of the shell. This example shows a highly anisotropic relativistic shell with larger azimuthal/polar than radial pressures. We note that the analytical and numerical solutions for relativistic finite shells found by [10] and [12] also have anisotropic pressures.

## 7 Discussion

In this work, we constructed families of potential-density pairs that represent spherical shells with finite thickness and shells with infinite thickness, but with

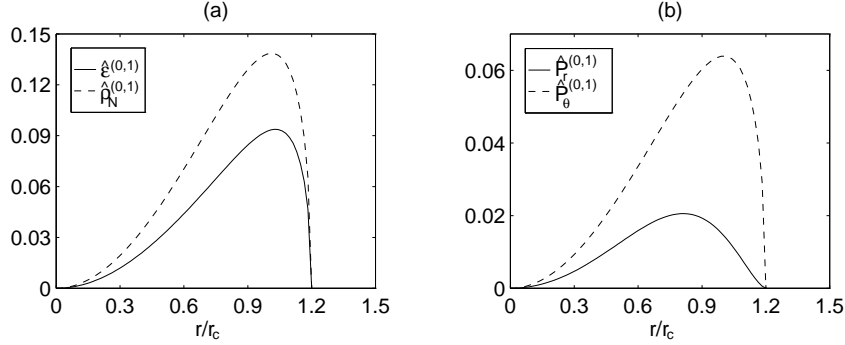


Figure 7: (a) The energy density  $\hat{\epsilon}^{(0,1)} = \epsilon^{(0,1)}/\rho_c$  (solid curve), equation (40), and the effective Newtonian density  $\hat{\rho}_N^{(0,1)} = \rho_N^{(0,1)}/\rho_c$  (dashed curve), equation (41), for the shell with  $\hat{a} = 1.2$ . (b) The radial pressure  $\hat{P}_r^{(0,1)} = P_r^{(0,1)}/(\rho_c c^2)$  (solid curve), equation (42), and the azimuthal/polar pressure  $\hat{P}_\theta^{(0,1)} = P_\theta^{(0,1)}/(\rho_c c^2)$  (dashed curve), equation (43), for the shell with  $\hat{a} = 1.2$ .

a hole at the centre. Shells with finite thickness were obtained by the superposition of spheres with finite radii, and shells with infinite extend by using the inversion theorem on spheres and finite shells. Furthermore, shells with finite thickness may be superposed to give a family of double shells with finite thickness. All the potential-density pairs discussed in this work can be expressed in terms of elementary functions. We also studied the rotation curves for these self-gravitating structures and made a stability analysis based on radial perturbations of circular orbits of individual particles. In all the examples discussed, we found stable structures.

A General Relativistic version of the Newtonian spherical potential-density pairs was obtained by using a particular isotropic form of a metric in spherical coordinates. We studied in some detail an example of a relativistic sphere and of a shell. In both cases, the matter presents equal azimuthal and polar pressures, but different from the radial pressure, and this anisotropy is a function of radius. It is possible to choose parameters such that all energy conditions are satisfied.

## Acknowledgments

D. V. thanks FAPESP for financial support, P. S. L. thanks FAPESP and CNPq for partial financial support.

## References

- [1] Plummer H. C., 1911, MNRAS, 71, 460
- [2] Jaffe W., 1983, MNRAS, 202, 995



- [3] Hernquist L., 1990, ApJ, 356, 359
- [4] Navarro J. F., Frenk C. S., White S. D. M., 1997, ApJ, 490, 493
- [5] Dehnen W., 1993, MNRAS, 265, 250
- [6] Tremaine S., Richstone D. O., Byun Y. I., Dressler A., Faber S. M., Grillmair C., Kormendy J., Lauer T. R., 1994, AJ, 107, 634
- [7] Zhao H. S., 1996, MNRAS, 278, 488
- [8] Bičák J., Schmidt B. G., 1999, ApJ, 521, 708
- [9] Rein G., 1999, Indiana Univ. Math. J., 48, 335
- [10] Andréasson H., 2007, Communications Math. Phys., 274, 409
- [11] Andréasson H., Rein G., 2007, Classical Quantum Gravity, 24, 1809
- [12] Gleiser R. J., Ramirez M. A., 2010, Classical Quantum Gravity, 27, 065008
- [13] Vogt D., Letelier P. S., 2010, MNRAS, 402, 1313
- [14] Kalnajs A. J., 1972, ApJ, 175, 63
- [15] González G. A., Reina J. I., 2006, MNRAS, 371, 1873
- [16] Morgan T., Morgan L., 1969, Phys. Rev., 183, 1097
- [17] Binney J., Tremaine S., 2008, Galactic Dynamics, 2nd edn. Princeton Univ. Press, Princeton, NJ
- [18] Thomson W. (Lord Kelvin), 1847, J. Math. Pures Appliquees, 12, 256
- [19] Kellog O. D., 1953, Foundations of Potential Theory, Dover Publications, New York
- [20] Letelier P. S., 2007, MNRAS, 381, 1031

## A Rotation curves and epicyclic frequency for spheres

The expressions for the circular velocity  $v_{c(m)}$  and epicyclic frequency  $\kappa_m$  for the spheres with  $m = 1, 2, 3, 4$  read as

$$v_{c(1)} = \sqrt{\frac{2GM}{\pi a^4}} \left[ \frac{a^4}{r} \arcsin\left(\frac{r}{a}\right) + \sqrt{a^2 - r^2} (2r^2 - a^2) \right]^{1/2}, \quad (46)$$

$$v_{c(2)} = \sqrt{\frac{2GM}{3\pi a^6}} \left[ \frac{3a^6}{r} \arcsin\left(\frac{r}{a}\right) - \sqrt{a^2 - r^2} (8r^4 - 14r^2a^2 + 3a^4) \right]^{1/2}, \quad (47)$$

$$v_{c(3)} = \sqrt{\frac{2GM}{15\pi a^8}} \left[ \frac{15a^8}{r} \arcsin\left(\frac{r}{a}\right) + \sqrt{a^2 - r^2} (48r^6 - 136r^4a^2 + 118r^2a^4 - 15a^6) \right]^{1/2}, \quad (48)$$

$$v_{c(4)} = \sqrt{\frac{2GM}{105\pi a^{10}}} \left[ \frac{105a^{10}}{r} \arcsin\left(\frac{r}{a}\right) - \sqrt{a^2 - r^2} (384r^8 - 1488r^6a^2 + 2104r^4a^4 - 1210r^2a^6 + 105a^8) \right]^{1/2}, \quad (49)$$

$$\kappa_1 = \sqrt{\frac{2GM}{\pi r^2 a^4}} \left[ \frac{a^4}{r} \arcsin\left(\frac{r}{a}\right) + \sqrt{a^2 - r^2} (10r^2 - a^2) \right]^{1/2}, \quad (50)$$

$$\kappa_2 = \sqrt{\frac{2GM}{3\pi r^2 a^6}} \left[ \frac{3a^6}{r} \arcsin\left(\frac{r}{a}\right) - \sqrt{a^2 - r^2} (56r^4 - 62r^2a^2 + 3a^4) \right]^{1/2}, \quad (51)$$

$$\kappa_3 = \sqrt{\frac{2GM}{15\pi r^2 a^8}} \left[ \frac{15a^8}{r} \arcsin\left(\frac{r}{a}\right) + \sqrt{a^2 - r^2} (432r^6 - 904r^4a^2 + 502r^2a^4 - 15a^6) \right]^{1/2}, \quad (52)$$

$$\kappa_4 = \sqrt{\frac{2GM}{105\pi r^2 a^{10}}} \left[ \frac{105a^{10}}{r} \arcsin\left(\frac{r}{a}\right) - \sqrt{a^2 - r^2} (4224r^8 - 13008r^6a^2 + 13624r^4a^4 - 5050r^2a^6 + 105a^8) \right]^{1/2}. \quad (53)$$

## B Potentials of inverted spheres

The expressions for the potentials  $\Phi_{m(inv.)}$  of the shells (15) with  $m = 1, 2, 3, 4$ , obtained by inversion of spheres, are

$$\Phi_{1(inv.)} = -\frac{GM}{8r} \left[ \frac{3r}{a} \arcsin\left(\frac{a}{r}\right) + \frac{\sqrt{r^2 - a^2}}{r^3} (5r^2 - 2a^2) \right], \quad (54)$$

$$\Phi_{2(inv.)} = -\frac{GM}{48r} \left[ \frac{15r}{a} \arcsin\left(\frac{a}{r}\right) + \frac{\sqrt{r^2 - a^2}}{r^5} (33r^4 - 26r^2a^2 + 8a^4) \right], \quad (55)$$

$$\Phi_{3(inv.)} = -\frac{GM}{384r} \left[ \frac{105r}{a} \arcsin\left(\frac{a}{r}\right) + \frac{\sqrt{r^2 - a^2}}{r^7} (279r^6 - 326r^4a^2 + 200r^2a^4 - 48a^6) \right], \quad (56)$$

$$\begin{aligned} \Phi_{4(inv.)} = -\frac{GM}{1280r} & \left[ \frac{315r}{a} \arcsin\left(\frac{a}{r}\right) + \frac{\sqrt{r^2 - a^2}}{r^9} (965r^8 - 1490r^6a^2 \right. \\ & \left. + 1368r^4a^4 - 656r^2a^6 + 128a^8) \right]. \end{aligned} \quad (57)$$

## C Potentials, rotation curves and epicyclic frequencies for spherical shells

The expressions for the potentials  $\Phi^{(m,n)}$  of the shells (24) with  $m = 0, 1$  and  $n = 1, 2$  are

$$\Phi^{(0,1)} = -\frac{G\rho_c\pi}{60a^3} \left[ \frac{15a^6}{r} \arcsin\left(\frac{r}{a}\right) - \sqrt{a^2 - r^2} (8r^4 - 6a^2r^2 - 17a^4) \right], \quad (58)$$

$$\begin{aligned} \Phi^{(0,2)} = -\frac{G\rho_c\pi}{3360a^5} & \left[ \frac{525a^8}{r} \arcsin\left(\frac{r}{a}\right) - \sqrt{a^2 - r^2} (240r^6 - 104r^4a^2 \right. \\ & \left. - 162r^2a^4 - 499a^6) \right], \end{aligned} \quad (59)$$

$$\begin{aligned} \Phi^{(1,1)} = -\frac{G\rho_c\pi}{1120a^5} & \left[ \frac{105a^8}{r} \arcsin\left(\frac{r}{a}\right) + \sqrt{a^2 - r^2} (80r^6 - 184r^4a^2 \right. \\ & \left. + 58r^2a^4 + 151a^6) \right], \end{aligned} \quad (60)$$

$$\begin{aligned} \Phi^{(1,2)} = -\frac{G\rho_c\pi}{20160a^7} & \left[ \frac{945a^{10}}{r} \arcsin\left(\frac{r}{a}\right) + \sqrt{a^2 - r^2} (896r^8 - 1712r^6a^2 \right. \\ & \left. + 264r^4a^4 + 394r^2a^6 + 1103a^8) \right]. \end{aligned} \quad (61)$$

We also give the expressions for the circular velocity  $v_c^{(m,n)}$  and epicyclic frequency  $\kappa^{(m,n)}$  for these members:

$$v_c^{(0,1)} = \sqrt{\frac{G\rho_c\pi}{12a^3}} \left[ \frac{3a^6}{r} \arcsin\left(\frac{r}{a}\right) + \sqrt{a^2 - r^2} (8r^4 - 2r^2a^2 - 3a^4) \right]^{1/2}, \quad (62)$$

$$v_c^{(0,2)} = \sqrt{\frac{G\rho_c\pi}{96a^5}} \left[ \frac{15a^8}{r} \arcsin\left(\frac{r}{a}\right) + \sqrt{a^2 - r^2} (48r^6 - 8r^4a^2 - 10r^2a^4 - 15a^6) \right]^{1/2}, \quad (63)$$

$$v_c^{(1,1)} = \sqrt{\frac{G\rho_c\pi}{32a^5}} \left[ \frac{3a^8}{r} \arcsin\left(\frac{r}{a}\right) - \sqrt{a^2 - r^2} (16r^6 - 24r^4a^2 + 2r^2a^4 + 3a^6) \right]^{1/2}, \quad (64)$$

$$v_c^{(1,2)} = \sqrt{\frac{G\rho_c\pi}{320a^7}} \left[ \frac{15a^{10}}{r} \arcsin\left(\frac{r}{a}\right) - \sqrt{a^2 - r^2} (128r^8 - 176r^6a^2 + 8r^4a^4 + 10r^2a^6 + 15a^8) \right]^{1/2}, \quad (65)$$

$$\kappa^{(0,1)} = \sqrt{\frac{G\rho_c\pi}{12r^2a^3}} \left[ \frac{3a^6}{r} \arcsin\left(\frac{r}{a}\right) + \sqrt{a^2 - r^2} (56r^4 - 2r^2a^2 - 3a^4) \right]^{1/2}, \quad (66)$$

$$\kappa^{(0,2)} = \sqrt{\frac{G\rho_c\pi}{96r^2a^5}} \left[ \frac{15a^8}{r} \arcsin\left(\frac{r}{a}\right) + \sqrt{a^2 - r^2} (432r^6 - 8r^4a^2 - 10r^2a^4 - 15a^6) \right]^{1/2}, \quad (67)$$

$$\kappa^{(1,1)} = \sqrt{\frac{G\rho_c\pi}{32r^2a^5}} \left[ \frac{3a^8}{r} \arcsin\left(\frac{r}{a}\right) - \sqrt{a^2 - r^2} (144r^6 - 152r^4a^2 + 2r^2a^4 + 3a^6) \right]^{1/2}, \quad (68)$$

$$\kappa^{(1,2)} = \sqrt{\frac{G\rho_c\pi}{320r^2a^7}} \left[ \frac{15a^{10}}{r} \arcsin\left(\frac{r}{a}\right) - \sqrt{a^2 - r^2} (1408r^8 - 1456r^6a^2 + 8r^4a^4 + 10r^2a^6 + 15a^8) \right]^{1/2}. \quad (69)$$

## D Potentials, rotation curves and epicyclic frequencies for inverted spherical shells

The expressions for the potentials  $\Phi_{(inv.)}^{(m,n)}$  of the inverted shells (26) with  $m = 0, 1$  and  $n = 1, 2$  are

$$\Phi_{(inv.)}^{(0,1)} = -\frac{G\rho_c\pi a^3}{60r} \left[ \frac{15r}{a} \arcsin\left(\frac{a}{r}\right) + \frac{\sqrt{r^2 - a^2}}{r^5} (17r^4 + 6a^2r^2 - 8a^4) \right], \quad (70)$$

$$\Phi_{(inv.)}^{(0,2)} = -\frac{G\rho_c\pi a^3}{3360r} \left[ \frac{525r}{a} \arcsin\left(\frac{a}{r}\right) + \frac{\sqrt{r^2 - a^2}}{r^7} (499r^6 + 162r^4a^2 + 104r^2a^4 - 240a^6) \right], \quad (71)$$

$$\Phi_{(inv.)}^{(1,1)} = -\frac{G\rho_c\pi a^3}{1120r} \left[ \frac{105r}{a} \arcsin\left(\frac{a}{r}\right) + \frac{\sqrt{r^2 - a^2}}{r^7} (151r^6 + 58r^4a^2 - 184r^2a^4 + 80a^6) \right], \quad (72)$$

$$\Phi_{(inv.)}^{(1,2)} = -\frac{G\rho_c\pi a^3}{20160r} \left[ \frac{945r}{a} \arcsin\left(\frac{a}{r}\right) + \frac{\sqrt{r^2 - a^2}}{r^9} (1103r^8 + 394r^6a^2 + 264r^4a^4 - 1712r^2a^6 + 896a^8) \right]. \quad (73)$$

The circular velocity  $v_{c(inv.)}^{(m,n)}$  and epicyclic frequency  $\kappa_{(inv.)}^{(m,n)}$  for these inverted shells read as

$$v_{c(inv.)}^{(0,1)} = \sqrt{\frac{4G\rho_c\pi a^3 (2r^2 + 3a^2)}{15r^3}} \left(1 - \frac{a^2}{r^2}\right)^{3/4}, \quad (74)$$

$$v_{c(inv.)}^{(0,2)} = \sqrt{\frac{4G\rho_c\pi a^3 (8r^4 + 12r^2a^2 + 15a^4)}{105r^5}} \left(1 - \frac{a^2}{r^2}\right)^{3/4}, \quad (75)$$

$$v_{c(inv.)}^{(1,1)} = \sqrt{\frac{4G\rho_c\pi a^3 (2r^2 + 5a^2)}{35r^3}} \left(1 - \frac{a^2}{r^2}\right)^{5/4}, \quad (76)$$

$$v_{c(inv.)}^{(1,2)} = \sqrt{\frac{4G\rho_c\pi a^3 (8r^4 + 20r^2a^2 + 35a^4)}{315r^5}} \left(1 - \frac{a^2}{r^2}\right)^{5/4}, \quad (77)$$

$$\kappa_{(inv.)}^{(0,1)} = \sqrt{\frac{4G\rho_c\pi a^3 (2r^4 + r^2a^2 + 12a^4)}{15r^7}} \left(1 - \frac{a^2}{r^2}\right)^{1/4}, \quad (78)$$

$$\kappa_{(inv.)}^{(0,2)} = \sqrt{\frac{4G\rho_c\pi a^3 (8r^6 + 4r^4a^2 + 3r^2a^4 + 90a^6)}{105r^9}} \left(1 - \frac{a^2}{r^2}\right)^{1/4}, \quad (79)$$

$$\kappa_{(inv.)}^{(1,1)} = \sqrt{\frac{4G\rho_c\pi a^3 (2r^6 + r^4a^2 + 27r^2a^4 - 30a^6)}{35r^9}} \left(1 - \frac{a^2}{r^2}\right)^{1/4}, \quad (80)$$

$$\kappa_{(inv.)}^{(1,2)} = \sqrt{\frac{4G\rho_c\pi a^3 (8r^8 + 4r^6a^2 + 3r^4a^4 + 265r^2a^6 - 280a^8)}{315r^{11}}} \left(1 - \frac{a^2}{r^2}\right)^{1/4}. \quad (81)$$

## E Potential, rotation curve and epicyclic frequency for a double shell

The potential  $\Phi_{(2)}^{(0,1)}$  of the double shell discussed in Section 5 reads as

$$\begin{aligned} \Phi_{(2)}^{(0,1)} = & -\frac{G\rho_c\pi}{20160a^7} \left\{ \frac{315a^{10}}{r} (7b^4 - 20b^2 + 16) \arcsin\left(\frac{r}{a}\right) \right. \\ & + \sqrt{a^2 - r^2} [-896r^8b^4 + 16r^6a^2b^2(17b^2 + 180) + 24r^4a^4(15b^4 - 52b^2 - 112) \\ & \left. + 2r^2a^6(289b^4 - 972b^2 + 1008) + a^8(1891b^4 - 5988b^2 + 5712)] \right\}. \quad (82) \end{aligned}$$

The corresponding expressions of the circular velocity  $v_{c(2)}^{(0,1)}$  and epicyclic frequency  $\kappa_{(2)}^{(0,1)}$  are

$$\begin{aligned} v_{c(2)}^{(0,1)} = & \sqrt{\frac{G\rho_c\pi}{960a^7}} \left\{ \frac{15a^{10}}{r} (7b^4 - 20b^2 + 16) \arcsin\left(\frac{r}{a}\right) \right. \\ & + \sqrt{a^2 - r^2} [384r^8b^4 - 48r^6a^2b^2(b^2 + 20) - 8r^4a^4(7b^4 - 20b^2 - 80) \\ & \left. - 10r^2a^6(7b^4 - 20b^2 + 16) - 15a^8(7b^4 - 20b^2 + 16)] \right\}^{1/2}, \quad (83) \\ \kappa_{(2)}^{(0,1)} = & \sqrt{\frac{G\rho_c\pi}{960r^2a^7}} \left\{ \frac{15a^{10}}{r} (7b^4 - 20b^2 + 16) \arcsin\left(\frac{r}{a}\right) \right. \\ & + \sqrt{a^2 - r^2} [4224r^8b^4 - 48r^6a^2b^2(b^2 + 180) - 8r^4a^4(7b^4 - 20b^2 - 560) \\ & \left. - 10r^2a^6(7b^4 - 20b^2 + 16) - 15a^8(7b^4 - 20b^2 + 16)] \right\}^{1/2}. \quad (84) \end{aligned}$$